SELF-TRANSPORT OF LIQUID DROPS THROUGH A FUNCTIONAL MESH FOR REMOVING SWEAT AWAY FROM SKIN

by

MANASVIKUMAR OZA

Presented to the Faculty of the Graduate School of
The University of Texas at Arlington in Partial Fulfillment
of the Requirements for the Degree of

MASTER OF SCIENCE IN MECHANICAL ENGINEERING

THE UNIVERSITY OF TEXAS AT ARLINGTON
December 2016

Acknowledgements

Words cannot be framed to convey my deepest gratitude and respect for my thesis advisor and committee chair, Professor Cheng Luo. His expertise in the field Micro/ Nano system, excellent guidance, patience motivated me to become an independent researcher and I am grateful for providing me with an excellent environment for doing research. Till this date, I have never seen a hardworking person like him and he is my biggest inspiration and he has always inspired me with innovative thoughts. I want to thank my thesis committee member Dr. Hyejin Moon and Dr. Zhen Xue Han, who dedicated their time to be on the committee and to guide me. I have been amazingly fortunate enough to work with you all.

I would also like to acknowledge the support of my colleagues Mr. Manjarik Mrinal, Mr. Mithun Ramanuj, Mr. Xiang Wang and all other colleagues during the progress of my thesis. I want to thank family for their endless love and for constantly motivating me to bring the best out of me. I want to thank my all friends and my roommates, who were with me through thick and thin.

Finally, I would like to dedicate this thesis to my father, Mr. Manharbhai and my mother, Mrs. Mandakini for their endless patience, motivation, and the countless sacrifices they made for providing me the best educational opportunities and this work was not possible without their constant love and encouragement.

December 2016

Abstract

SELF-TRANSPORT OF LIQUID DROPS THROUGH A FUNCTIONAL MESH FOR REMOVING SWEAT AWAY FROM SKIN

Manasvikumar Oza, MS

The University of Texas at Arlington, 2016

Supervising Professor: Cheng Luo

In this work, a functional mesh is developed to transport liquid drops from one side of the mesh to the other. A theoretical model is established, which has been used to obtain three design criteria. Based on these design criteria, functional meshes have been generated and tested with commercially available sponge attached to the mesh. Finally, such a mesh is demonstrated to be effective to remove sweat from human skin. As an application of this research, the concept of this functional mesh solves existing problems with a sport wear. The current sport wear is capable of absorbing sweat, but not transporting it away from the skin. This concept can also be used at the surface of contact of prosthetic parts and body parts. i.e. Joints at artificial arm or artificial legs, as mesh can transfer sweat from the skin to the outer surface of a sport wear or joint of prosthetic part, keeping the interface between the wear and skin dry.

Table of Contents

List of Illustrations

Chapter 1 Introduction

One of the most natural phenomena, the water flows towards gravity which implies a scientific principle, i.e., the gravitational potential energy of water is instinctively be converted into kinetic energy. Practically water can be continuously lifted against gravity only with external driving factors, such as the transpiration of giant plants, negative pressure supplied by a sectorial proboscis of butterflies and open-close motion of the shorebirds mouthpart with a capillary ratchet [1].

Taking an interest in self-transport water, in 1992, a self-propelling millimeter-scale uphill run of water drops was achieved on the functional silicon wafer with a wettability gradient [2], which can be attributed to the asymmetrical Laplace pressure. Other methods for water drop movement like wettability gradient [3], geometrical shape, [4] and other external stimuli [5] are also topic of interest for researchers.

Recently, a group of researchers succeeded to create a superhydrophobic pump which can transfer water continuously and spontaneously even in the opposite direction of gravity. For the pump to work continuously, they kept some water in the tube initially. The superhydrophobic pump was constructed by the copper mesh and polymer tube with contact angle of 90^0. The copper mesh was covered with superhydrophobic material. Here, the concept of self-transporting water is dependent on the capillarity of the upper tube. Copper fiber Superhydrophobic mesh can transfer the water to the tube and hold it in the tube till certain height. The maximum ascending height is depends on wettability of the mesh, drop diameter and inner diameter of the tube [6].

Another fascinating phenomenon focusing on the self-transportation of a liquid is with the micropatterns. Three dimensional liquid flows can be transported on a micropatterned superhydrophobic textile (MST) platform. Specifically, the MST system uses the surface tension encouraged Laplace pressure to enable the liquid motion along the hydrophilic material, in addition to the capillarity present in the fibrous structure. The fabrication of MST is simply accomplished by stitching hydrophilic cotton into a superhydrophobic fabric substrate, from which well-controlled wetting patterns are established for interfacial microfluidic operations [7]. The three-dimensional flow patterns can gather small drops in one place and make bigger drop which can be removed easily.

Some of the researchers used polydimethylsiloxane (PDMA) membrane as a base of absorbing or transporting liquid. They have used micropores of the PDMA to govern capillary action. In this research, they have made a thin soft Janus PDMS film with opposing porous and nonporous faces was fabricated and tested for qualities applicable to improve current bandages, such as porosity, stretch ability, and water wettability [8]. They made a dressing material that can replace a bandage and can be used for wound care and drug delivery applications. This dressing has two parts, first one is in contact with wound surface which is primary dressing while secondary dressings cover the primary dressing to support and hold it in place [9].

Getting motivation from these researches, a capillary action can be used as the fundamental principle. Capillary action is the ability of a liquid to flow in narrow spaces without the assistance of, or even in opposition to external forces. It occurs because of intermolecular forces between the liquid and surrounding solid surfaces. The combination of surface tension and adhesive forces between the liquid and container wall act to propel the liquid [10].

For this research, a stainless-steel mesh is used which is commercially available and bought from TWP Inc. A superhydrophilic coating is used to make one side of the mesh more hydrophilic. The micropores propel water drops while different wetting regions of the mesh force the water drops to move to the top surface of the mesh and hold it there. Titanium oxide (TiO_2) is used as a superhydrophilic coating purchased from

Sigma-Aldrich Co. LLC, whose contact angle is 0^o [11]. TiO_2 is biocompatible material, and it can be used as a super hydrophilic coating material [12]. Accordingly, it is adopted as the coating material. The bottom portions of the meshes are not treated, and remain hydrophobic.

Chapter 2 Theoretical Background and Modeling

2.1 Two requirements about a desired mesh

Microchannels and micropillars are often applied as structures to enhance surface hydrophobicity or hydrophilicity [13,14,17-27]. In our case, a mesh consists of micropores. There are two requirements about a functional mesh. First, when a liquid drop is located on the bottom side of the mesh (fig. 2-1a), this mesh should enable the drop to self-transport to the top side of the mesh (fig. 2-1b). Second, after the transport, the bottom of the drop should be suspended between mesh fibers, but not below the bottom side of the mesh.

2.2 Design according to the first requirement

A two-dimensional model is established here to design the mesh according to these two requirements. Obviously, when these two sides have the same wetting properties, due to symmetry in geometry and wetting, it is impossible for a liquid drop to self-transport from the bottom to the top side of the mesh. Also, it is known that a liquid drop prefers to move from a less wetting region to a more wetting area.

Next, we consider the first requirement. That is, we first consider whether a liquid drop would change its configuration from Figure 2-1a to Figure 2-1b. As illustrated in Figure 2-1a, let $A_1A_2A_3$ denote the cross-sectional profile of the air/liquid interface at the drop bottom, while use $B_1B_2B_3B_4$ to represent the profiles of the drop top. Assume that the height of an interface is less than its capillary length, which is 2.7 mm for water. Accordingly, the gravity effect on the drop can be neglected [17,18], and liquid pressure thus has a uniform distribution along the interface. Furthermore, $A_1A_2A_3$, B_1B_2, and B_3B_4 can be approximated as circular arcs [20].

Use θ_1 and θ_2 to be equilibrium contact angles on the bottom and top portions of a mesh fiber. The top portion refers to part of the top half surface of the fiber, while the bottom the rest of the fiber surface (fig. 2-1a). In our design, θ_2 is less than 90º, while $\theta_1 > \theta_2$. That is, the top portion of the mesh is lyophilic, and the bottom less lyophilic (fig. 2-1a). If the sidewalls of the fiber are smooth, then θ_1 and θ_2 are intrinsic contact angles. Otherwise, they are apparent contact angles. Let γ represent surface tension of liquid. Set p_a and p_w to be atmospheric pressure and pressure inside the liquid drop, respectively. $(p_w - p_a)$ is so-called Laplace pressure. According to Young-Laplace equation [27], p_w is related to γ by

$$p_w = \gamma(\frac{1}{R_1} + \frac{1}{R_2}) + p_a, \tag{1}$$

where $\frac{1}{R_1}$ and $\frac{1}{R_2}$ denote two principal curvatures of the air/liquid interface, and R_1 and R_2 are the radii of the two principal curvatures, respectively. In practice, after a liquid drop is placed on the back side of a micropore-formed surface, the bottom profile of the drop has a spherical shape. Since this profile bends towards the air, its two principal curvatures are positive. Let p_{w1} denote liquid pressure at $A_1A_2A_3$. Accordingly, by Eq. (1), p_{w1} is larger than p_a.

The fibers will be chosen to have small radii. Consequently, due to the initial speed of the liquid drop when it is put on the mesh, $B_1B_2B_3B_4$ will reach the top portions of the fibers. Set p_{w2} to be liquid pressure at B_1B_2 and B_3B_4. Since the top portions are lyophilic, these interfaces bend towards the drop (fig. 2-1a). Hence, their principal curvatures are negative. Subsequently, by Eq. (1), p_{w2} is less than p_a. Thus, we have (p_{w1} - p_{w2})>0. This pressure difference should drive the liquid to further move up to the top side of the mesh (fig. 2-1b).

In the final configuration (fig. 2-1b), let $b_1b_2b_3$ denote the cross-sectional profile of the air/liquid interface on the drop top, while use $a_1a_2a_3a_4$ to represent the profiles on the bottom side. $a_1a_2a_3a_4$ is located below the top portions of the fibers. Set l_1 to be the distance between b_1 and b_3. Let h denote the deflection of a_1a_2 at its middle point. It is also the maximum deflection of a_1a_2. Another possible final configuration is given in figure 2-1c, in which $a_1a_2a_3a_4$ is located on the top portions. In this configuration, since $b_1b_2b_3$ and $a_1a_2a_3a_4$ bends towards air and drop, respectively, p_{w1} and p_{w2} are less and greater than p_a, separately. Accordingly, we have (p_{w1} - p_{w2})<0. Hence, the liquid drop is not stationary in the corresponding configuration. Subsequently, $a_1a_2a_3a_4$ has to move downwards, changing to the configuration shown in figure 2-1b. In addition, we desire to make $a_1a_2a_3a_4$ move upwards as much as possible such that more liquid is transported to the top side of the mesh. Hence, the lyophilic portion is not extended to the bottom portion of a fiber, and the configuration shown in figure 2-1b is the desired one.

Furthermore, we determine the coverage of the lyophilic coating, as well as the location of $a_1a_2a_3a_4$ in the final configuration. Let o denote the center of a fiber (fig. 2-2a). Set l to be the space between two neighboring fibers, and let r denote the radius of the fiber. Without loss of generality, let's focus on a_1a_2. The same analysis will be applied to a_3a_4 as well. Set φ to be the angle formed by oa_1 and vertical line (fig. 2-2a), and $0 < \varphi <$ 360°. Then, we have [20]

$$p_{w1} = \frac{-2\gamma \sin(\theta_1 + \varphi)}{(l + r - r\sin\varphi)} + p_0 \,. \tag{2}$$

Set φ_0 and φ_1 to be the values of φ when p_{w1} equals p_0 and its maximum value, respectively. Use c_0 and c_1 to represent the corresponding points on the perimeter of the fiber (Fig. 2a). It follows from Eq. (2) that

$$\varphi_0 = 180^{\circ} - \theta_1, \tag{3}$$

$$\varphi_1 = 270^{\circ} - \theta_1. \tag{4}$$

Let $p_{w1\max}$ denote the maximum value of p_{w1}. By Eq. (2), we get

$$p_{w1\max} = \frac{2\gamma}{(l + r + r\cos\theta_1)} + p_0. \tag{5}$$

According to the value of θ_1, there exist two cases.

Case I: θ_1 is larger than 90º, i.e., the bottom portion is lyophobic (fig. 2-2a). In this case, by Eqs. (3) and (4), c_1 is located on the bottom half of the fiber, while c_0 is on the top half (fig. 2-2a). Let c_2 represent the lowest point on the perimeter. The corresponding value of φ at this point is 180º. As φ changes from 180º to φ_1, i.e., when a_1 moves from c_2 to c_1 during the process that a liquid drop transports from the bottom to the top side of the mesh, p_{w1} increases from $(\frac{2\gamma\sin\theta_1}{l + r} + p_0)$ to the maximum value of $(\frac{2\gamma}{l + r + r\cos\theta_1} + p_0)$. As φ further varies from φ_1 to φ_0, i.e., when a_1 further moves from c_1 to c_0, p_{w1} decreases from $(\frac{2\gamma}{l + r + r\cos\theta_1} + p_0)$ to p_0. Meanwhile, we have

$$p_{w2} = \frac{2\gamma \sin\theta}{l_1} + p_0, \tag{6}$$

Where, θ is the apparent contact angle that $b_1b_2b_3$ forms with the mesh surface. Since the top portion of the mesh is lyophilic, θ should be less than θ_2 [13]. Also, by Eqs. (5) and (6), p_{w2} is smaller than $p_{w1\max}$, but larger than p_0. Furthermore, noting that $l_1>(l+r)$ and that $\theta<\theta_1$, p_{w2} is smaller than $(\frac{2\gamma\sin\theta_1}{l+r}+p_0)$. Accordingly, a_1 should eventually be stationary at a point between c_0 and c_1 (fig. 2-2a). At the corresponding position, p_{w1} equals p_{w2}. Consequently, only the part of the fiber surface that is located above c_0 is set to be lyophilic.

Case II: θ_1 is less than 90º, i.e., the bottom portion is also lyophilic (fig. 2-2b). In this case, by Eqs. (3) and (4), c_0 and c_1 are located on the two sides of c_2 (fig. 2-2b). As φ changes from 180º to φ_0, p_{w1} decreases from $(\frac{2\gamma\sin\theta_1}{l+r}+p_0)$ to p_0. Since p_{w2} is still smaller than $(\frac{2\gamma\sin\theta_1}{l+r}+p_0)$, a_1 should eventually be stationary at a point between c_0 and c_2 (fig. 2-2b). At the corresponding position, p_{w1} equals p_{w2}. As in Case I, only the part of the fiber surface that is located above c_0 is set to be more lyophilic.

2.3 Design according to the second requirement

Noting that the liquid pressures at a_1a_2 and $b_1b_2b_3$ are equal, according to Eq. (4) of [20], we have

$$h = \frac{1}{2}(R - \sqrt{R^2 - l^2}), \tag{7}$$

where R denotes radius of $b_1b_2b_3$. R can be increased by reducing θ through the introduction of a small θ_2. When $\theta_2 \rightarrow 0^{\circ}$, we have $\theta \rightarrow 0^{\circ}$. Accordingly, $R \rightarrow \infty$. This result has two implications. First, by Eq. (7), $h \rightarrow 0.$ Thus, a_1a_2 should not deflect beyond the bottom side of the mesh in either case considered in Sub-section 2.2. That is, the second requirement is satisfied in both cases. Second, by Eq. (1), both p_{w1} and p_{w2} equal p_0. Thus, a_1 is located at c_0 in either case.

Based on the analysis of Sub-sections 2.2 and 2.3, three design criteria are obtained. First, the coating on the top portion of the mesh should be highly lyophilic. Second, the bottom portion of the mesh should be less lyophilic. Third and finally, both fiber diameters and pore sizes should be much smaller than a drop size such that a liquid drop could easily reach the top portion of the fiber from the bottom side of the mesh.

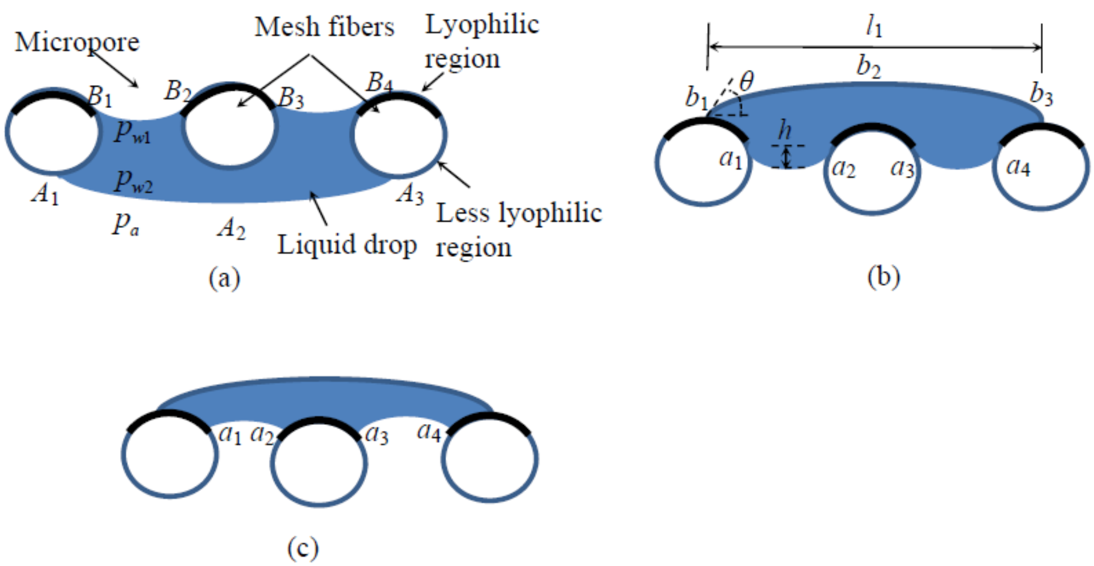

Figure 2-1. Schematics (side view) of (a) initial configuration, in which a liquid drop is placed on the bottom side of a mesh, (b) final configuration, in which the drop transports to the top side of the mesh, and (c) another possible final configuration (not to scale).

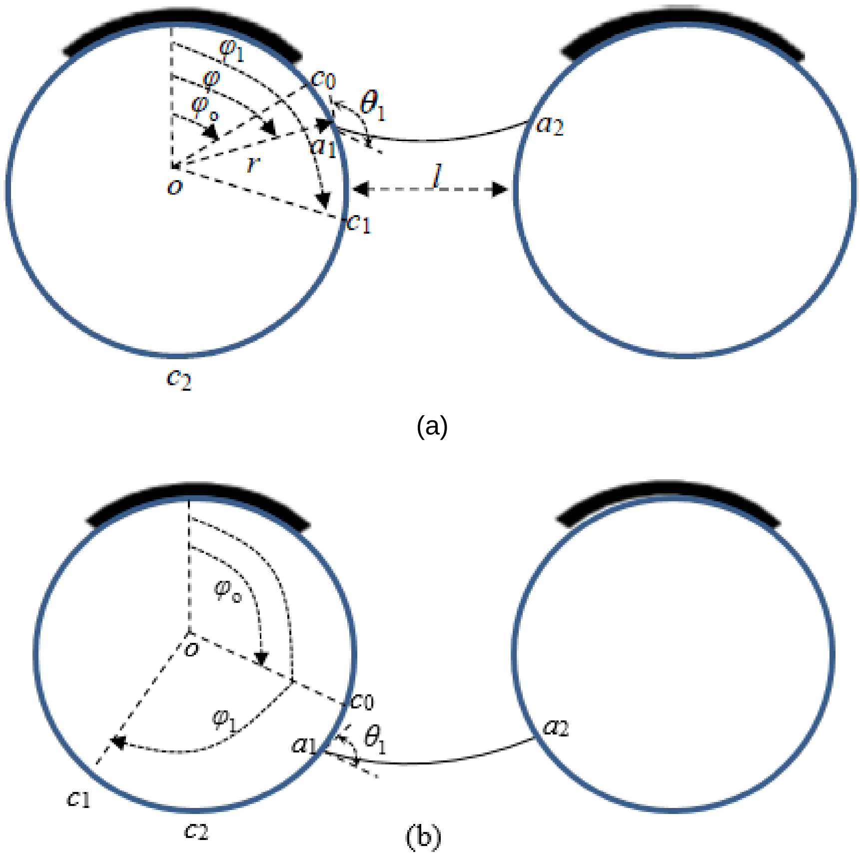

Figure 2-2 Schematic (side view) of the lower air/water interface between two fibers in the final configuration, when the bottom portion is (a) lyophobic, or (b) lyophilic (not to scale).

Chapter 3 Experimental Design and Methods

3.1 Contact angles of mesh fiber

Receding and advancing contact angles were measured using a similar approach as shown in figure 3-1, a mesh fiber was inserted into water. When the fiber was stationary inside water, an equilibrium contact angle of water on the fiber was observed through an optical microscope. The pictures of air/water interfaces were subsequently taken using Manistee software of the ScopeTek Company. The contact angles of these interfaces with the fiber surface were then determined using MB-Ruler software of the Dance Patterns Company. The receding and advancing angles of the air/water interface on the mesh fiber were measured by slightly moving the fiber up and down in the solution. In this work, three measurements were taken for each contact angle with an error of 2^{o}. The mean values of the contact angles are given in figure 3-1 and figure 3-2 that were measured on representative samples.

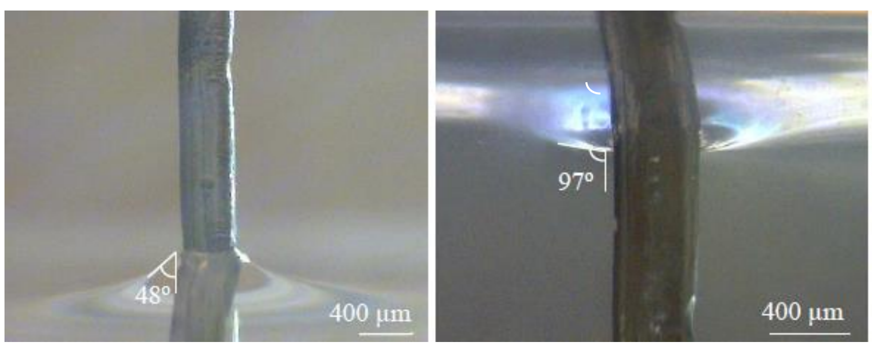

(a) (b)

Figure.3-1 (a) receding angle of untreated mesh fiber, (b) advancing angle of untreated mesh fiber

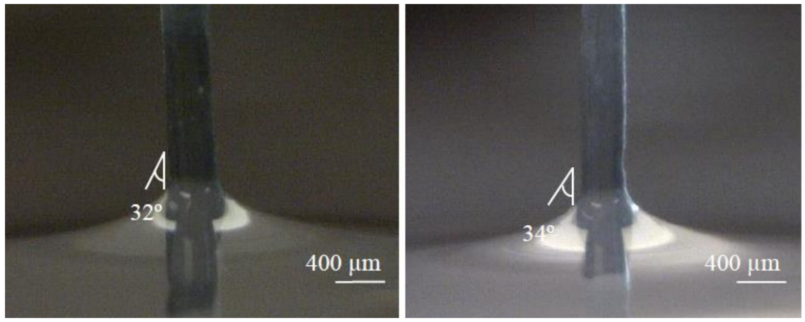

(a) (b)

Figure 3-2 (a) receding angle of TiO_2 coated mesh fiber, (b) advancing angle of TiO_2 coated mesh fiber

These experiments show that untreated mesh has hydrophilic surface, and have a receding and advancing angle of 48^0 and 97^0, respectively. While TiO_2 coated mesh has superhydrophilic surface, and have a receding and advancing contact angle of 32^0 and 34^0, respectively.

In this research TiO_2 (Titanium oxide) was used as a super hydrophilic coating. Solution of TiO_2 Nano powder and methanol with the ratio of 1.5 gm in 20 ml, respectively is coated on the mesh using a fine mist spray. According to the design criteria given in section 2.2 and 2.3, top sides of the meshes are covered with TiO_2 coating, while the bottom portions of the meshes kept untreated.

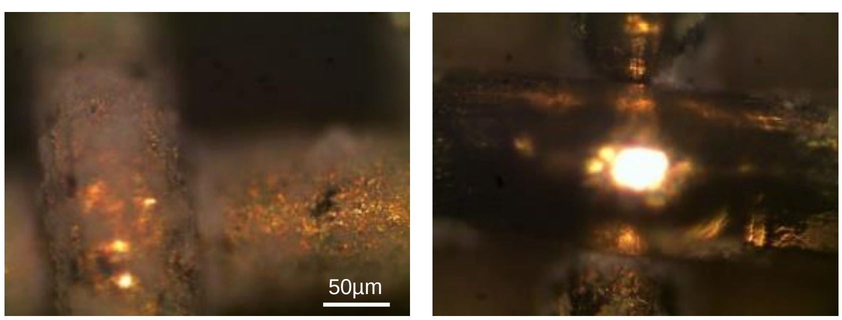

(a) (b)

Figure 3-3 Stainless steel mess coated with TiO_2 (a) top surface of the mesh, (b) bottom surface of the mesh

3.2 Mesh selection

Four kinds of the stainless-steel mesh were tested to choose best one of them with the same type of coating. They have pore sizes of 84, 140, 304 and 660 µm, respectively and fiber diameter of 20, 100, 310 and 430 µm, respectively. For simplicity, thereafter, they are referred to as 84-, 140-, 304- and 660-meshes. These meshes had hydrophilic surface on bottom side and superhydrophilic surface on top side.

From the experiments, Pore size with equal to or less than140 µm works good. Thus, for the further experiments I decided to use a mesh with pore size of 140 µm.

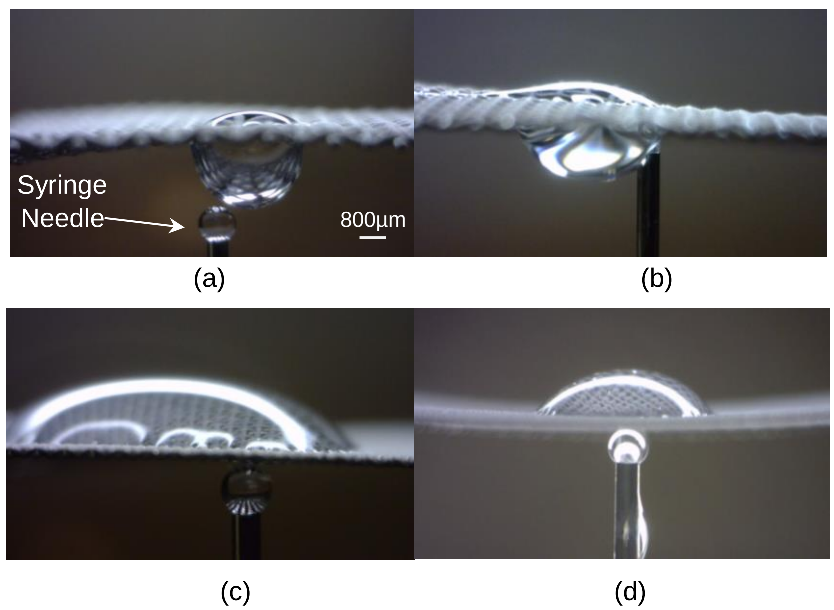

Figure 3-4 (a) 660- mesh, (b) 304- mesh, (c) 140- mesh, (d) 84- mesh

3.3 Experimental Setups

Five types of tests were conducted on mesh and after that the samw mesh was tested on the skin. In the first two types of experiment, water was supplied, using a syringe needle (fig. 3-5a) and a moving base (fig. 3-5b), respectively. The third type had a similar setup as the first (fig. 3-5c). The only difference was that a sponge was attached to the top side of the mesh. In the fourth and fifth types of experiments mesh was placed vertically and like second and third experiment water drops were supplied from horizontal needle (fig. 3-5d) and a vertical moving base (fig. 3-5e), respectively. Finally, in the sixth type, mesh was used to remove water drops from skin.

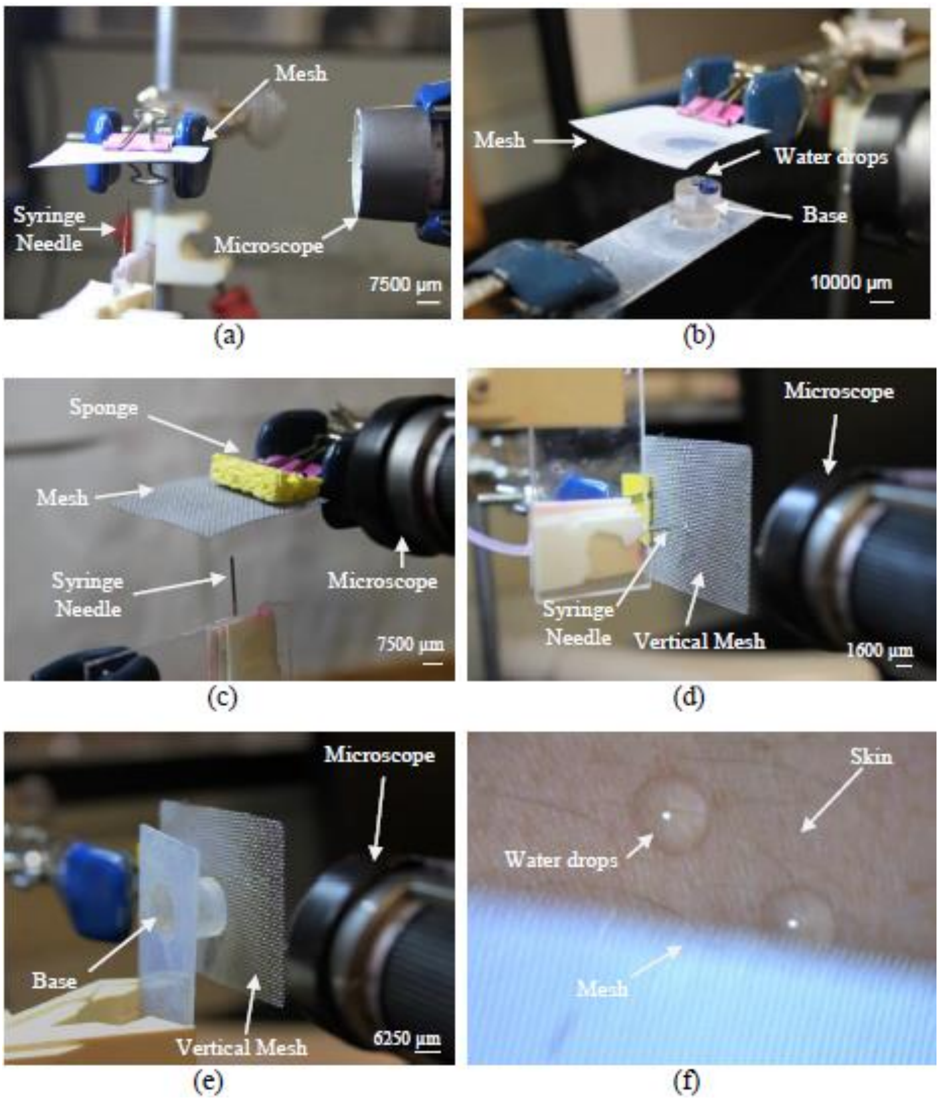

Figure 3-5 Six experimental setups with (a) shooting of water drops from a syringe needle, (b) using a moving base, (c) sponge attached on the top side of a functional mesh, (d) vertically shooting of water drops from the needle, (e) using vertical moving base, (f) water drop put on the skin absorbing with the functional mesh

Chapter 4. Experimental Results

4.1 Comparison and testing of the coating over a mesh

In these experiment tests, syringe needle was used to supply continuous water drops. For the sake of comparison two types of meshes with the pore size of 140 µm and 660 µm are used. Here for the first and second test, 140- mesh (fig. 4-1a) and 660-mesh fig. 4-1a) were used. Both the meshes were left untreated. These meshes can't hold the water drops because of the same wetting property on both sides of the mesh. Third test was done with the 140- mesh. This mesh was coated with TiO_2 on both side of the mesh. This mesh can hold the water drops and spread it over the mesh surface because of its hydrophilic wetting property (fig. 4-1 c), but later it continues shooting of the water drops from the syringe needle, bigger water drop started forming on bottom surface of the mesh which deflect beyond the bottom surface of the mesh.

Next test was same as last one but with the 660- mesh. Both sides of mesh were coated with TiO_2 (fig. 4-1 d). Due to the bigger fiber diameter, water drop is not able to get much contact surface. So, this mesh is not able to hold the water drops on it. 140- mesh was used in last and fifth test and coated with the TiO_2 on top side of the mesh. This mesh works great because it fulfills the requirement which is derived in the theory, top side of the mesh coated with TiO_2 which makes top surface more hydrophilic (fig. 4-1 e), which can hold the water drops on top surface the mesh.

After the comparison (fig. 4-2) of 140-micron mesh, one with TiO_2 coated on the top side (fig. 4-2a) and another is both the side coated with TiO_2 (fig. 4-2b), it is clear that first one is better, which is needed for certain application. So, 140-micron pore sized mesh coated with TiO_2 on the top side was used for the further experimental tests.

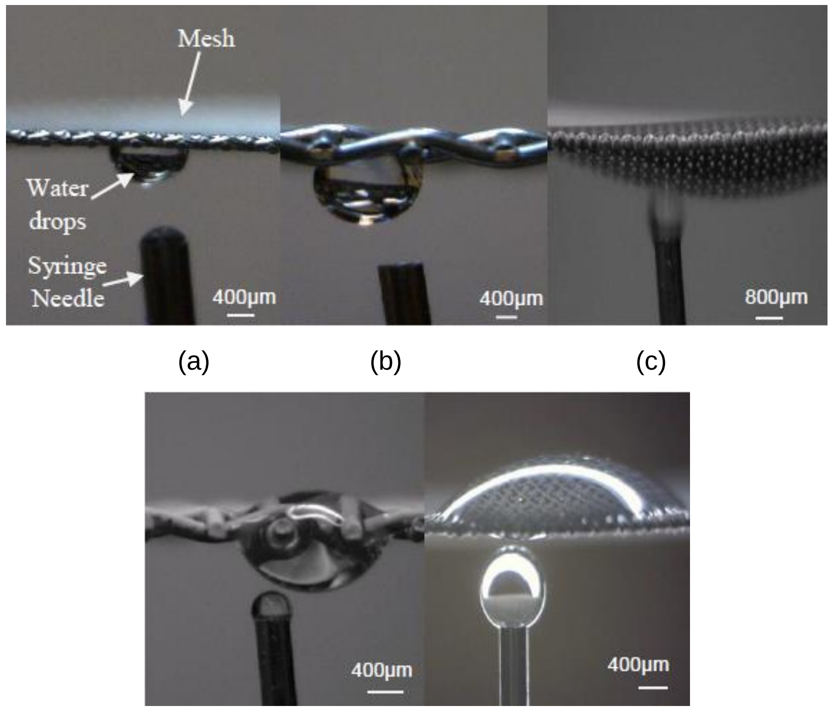

Figure 4-1 Water drops on: (a) uncoated140-mesh, (b) uncoated 660-mesh, (c) 140-mesh whose both sides were coated with TiO_2, (d) 660-mesh whose both sides were coated with TiO_2, and (e) 140-mesh, whose top side was coated with TiO_2

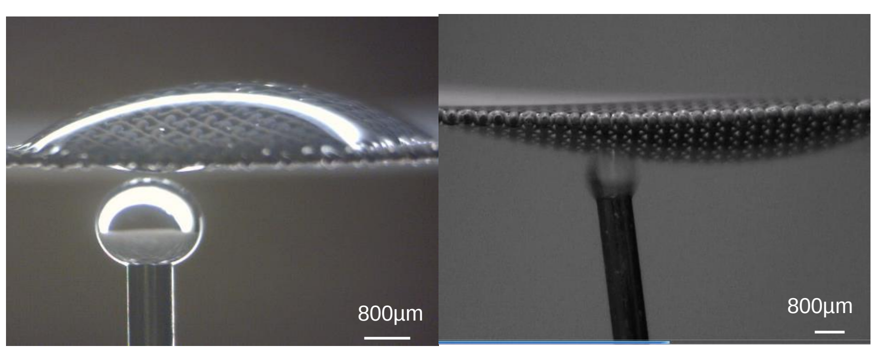

(a) (b)

Figure 4-2 140-micron mesh (a) one side coated with TiO_2 (b) both side coated with TiO_2

4.2 Six types of experimental test

First two tests were conducted to check if the mesh could hold the continuous water drops or not. First and second experiment setups were used for first two test with 140- mesh coated with TiO_2 on the top. In the first test (fig.4-3) syringe needle was used for continues shooting of water drop on the bottom surface of the mesh, while for the second test (fig.4-4), a cylinder base was used for continues delivery of the water drops. An average water drop volume from the syringe is 23 μl while, volume of the water drop which moving base supplied to the mesh is 26 μl. Continues drops from syringe were absorbed and hold on top surface (fig.4-3 b) which makes a big water drop (fig. 4-3 c) on the top surface. In the test with the moving base, it is moving up (fig 4-4 b) and down (fig 4-4 c) to get contact between water drop on base and bottom surface of the mesh, similar to first experiment big water drop form on the top surface of the mesh (fig 4-4 d).

Next test was with the third experimental setup which was same as the first one. Just a difference was a sponge attached to the mesh as a second layer of the mesh (fig. 4-5a). Here mesh absorbed and held the drop on the top surface (fig. 4-5b) until it made the big drop (fig. 4-5c), then after big drop moved towards the sponge which absorbs the water (fig. 4-5d).

Sponge size before absorbing the water was 5 × 30 × 16.10 mm and after maximum water absorption sponge size was 9.20 × 30 ×16.10 mm. Sponge weight before absorbing the water and after maximum water absorption was 0.25 gm and 4.50 gm, respectively. The maximum amount of water absorbed by the sponge was 4.23 ml.

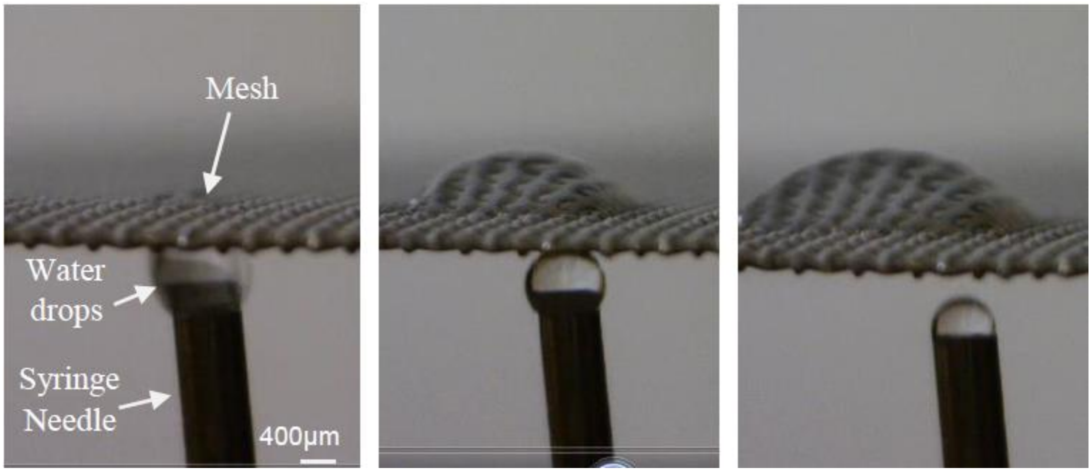

(a) (b) (c)

Figure 4-3 Continuous shooting of water drops from the syringe needle to one side TiO_2 coated 140- mesh.

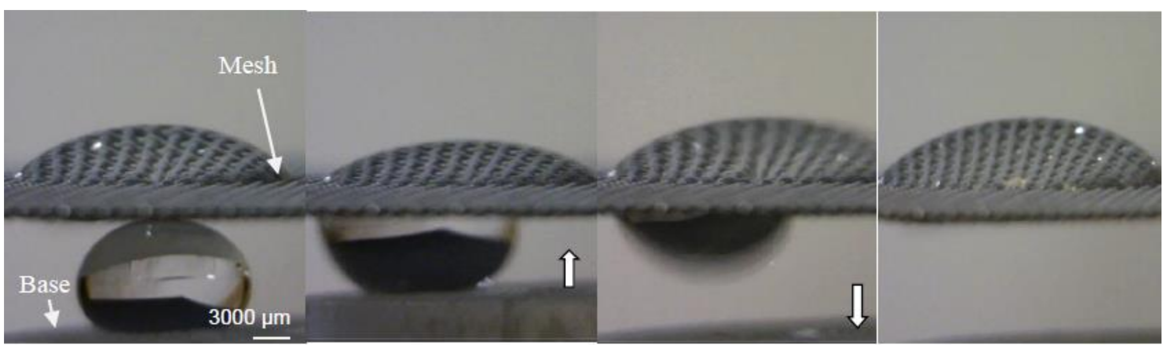

(a) (b) (c) (d)

Figure 4-4 (a) water drop on base moving towards the 140- mesh, (b) water drops getting contact with the mesh as base moving upward, (c) drops transferring to other side as base, (d) bigger water drops form on the top surface

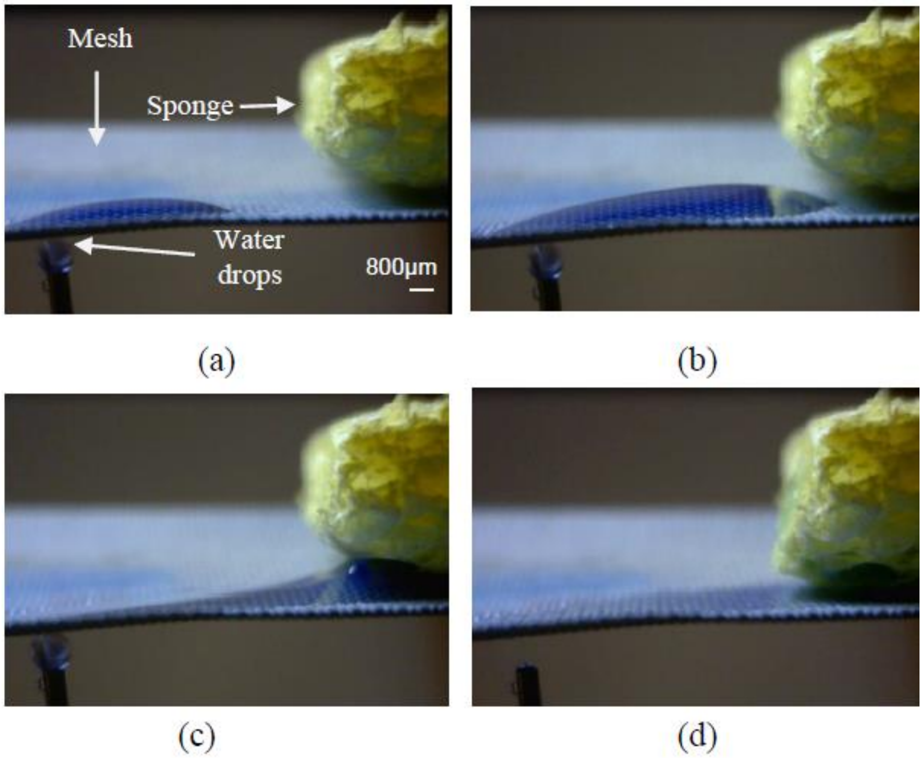

Figure 4-5 (a) small water drops were supplied from a syringe needle to 140-mesh, whose top side was covered with TiO_2, (b) the drops transported to the top side of the mesh, (c) a big drop slid towards a sponge over the mesh, and (d) the sponge absorbed the large drop that was formed on the top of the mesh

In the next two tests, mesh is vertically oriented to check whether water drain down by gravity. For third and fourth tests, horizontal syringe needle (fig. 4-6) and vertical base (fig. 4-7) were used, respectively to supply the water drops. A big water drop was formed on the other side of mesh because of continuous shooting from the horizontal syringe needle and moving base. Due to the gravitational force, a big drop started moving in a direction of the gravity.

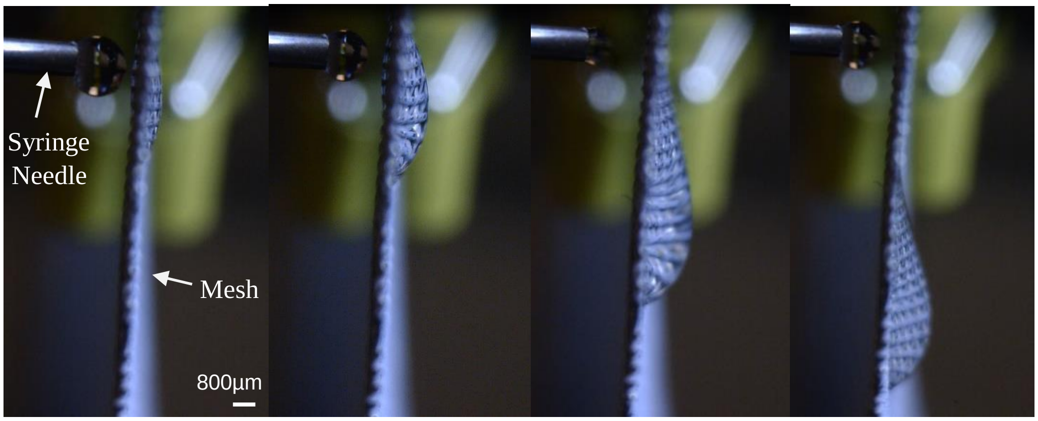

(a) (b) (c) (d)

Figure 4-6 (a) shooting water drop from the horizontal syringe needle on vertical mesh, (b,c) forming bigger water drops on the mesh from continues shooting, (d) bigger drops started moving downwards due to gravity force.

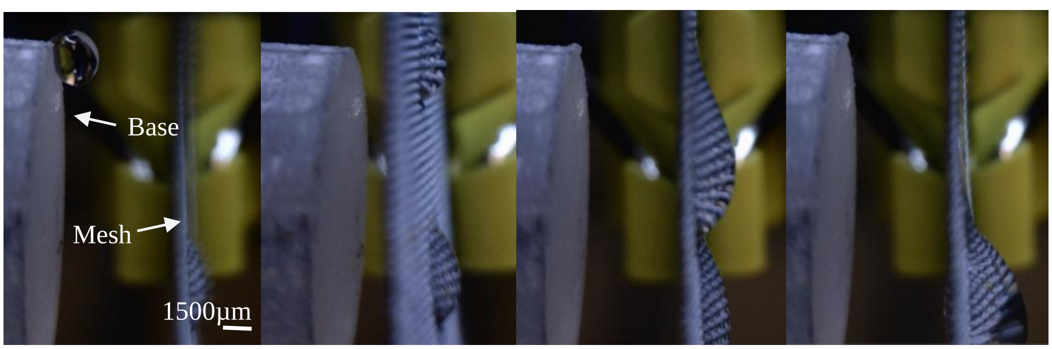

(a) (b) (c) (d)

Figure 4-7 (a) water drop on vertical base moving towards the 140- mesh, (b) water drops getting contact with the mesh as drops delivered one by one, (c) bigger drops started moving on other side of the mesh, (d) because of the gravity, drops started moving down.

Three water drops were placed on a skin to simulate a sweat over a skin, a 140-mesh, whose top side was covered with TiO_2, was contact over the drops and the drops were transported to the top side of the mesh and the water drops were removed from the skin using the mesh.

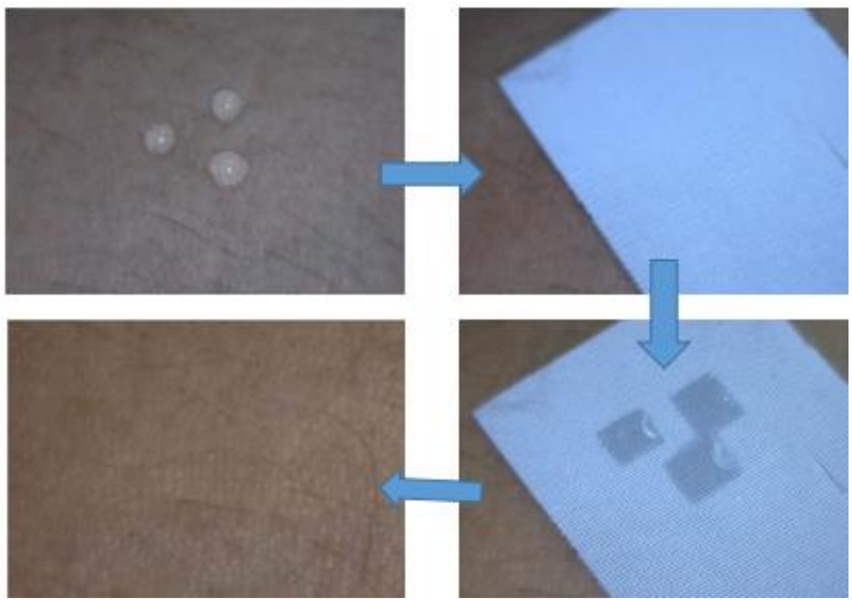

Figure 4-8 Three water drops were put on skin.

Chapter 5 Summary and Conclusions

In this work, we have designed a functional mesh through theoretical and experimental investigations to transport water drops from its bottom side to the top. The top side of the mesh is coated with a highly hydrophilic material, while the bottom is hydrophilic. The pore sizes of 140 μm or less can work for this concept. This functional mesh can be considered as a prototype of the mesh structure in a new sport wear, which is capable of not only absorbing sweat but also transporting it away from the skin.

Future work

- This research can be extended further by testing on textiles and using other superhydrophilic materials.

- Another application can be the use of mesh with sponge on surface of prosthetic parts like artificial arm or artificial leg to remove the sweat from the joint at body part and prosthetic part.

References

[1] a) W. T. Pockman , J. S. Sperry , J. W. Oleary , Nature 1995 , 378 , 715 ;(b) M. A. Zwieniecki , P. J. Melcher , N. M. Holbrook , Science 2001 ,291 , 1059 ; (c) M. Prakash , D. Quéré , J. W. M. Bush , Science 2008 ,320 , 931 ; d) H. W. Krenn , Annu. Rev. Entomol. 2010 , 55 , 307 .

[2] M. K. Chaudhury , G. M. Whitesides , Science 1992 , 256 , 1539 .

[3] a) S. Daniel , M. K. Chaudhury , J. C. Chen , Science 2001 , 291 , 633 ;(b) S. C. Hernandez , C. J. C. Bennett , C. E. Junkermeier , S. D. Tsoi ,F. J. Bezares , R. Stine , J. T. Robinson , E. H. Lock , D. R. Boris ,B. D. Pate , J. D. Caldwell , T. L. Reinecke , P. E. Sheehan ,S. G. Walton , ACS Nano 2013 , 7 , 4746 ; c) H. Zhou , H. X. Wang ,H. T. Niu , T. Lin , Sci. Rep. 2013 , 3 , 2964 ; d) J. Wu , N. Wang ,L. Wang , H. Dong , Y. Zhao , L. Jiang , Soft Matter 2012 , 8 , 5996 ; e) M. Y. Cao, J. S. Xiao, C. M. Yu, K. Li, L. Jiang, Small 2015 ,DOI:10.1002/smll.201500647.

[4] a) E. Lorenceau , D. Quéré , J. Fluid Mech. 2004 , 510 , 29 ;(b) Y. M. Zheng , H. Bai , Z. B. Huang , X. L. Tian , F. Q. Nie , Y. Zhao , J. Zhai , L. Jiang , Nature 2010 , 463 , 640 ; c) J. Ju , H. Bai , Y. M. Zheng , T. Y. Zhao , R. C. Fang , L. Jiang , Nat. Commun. 2012 , 3 , 1247 .

[5] a) K. Ichimura , S. K. Oh , M. Nakagawa , Science 2000 , 288 ,1624 ; b) T. A. Duncombe , E. Y. Erdem , A. Shastry , R. Baskaran , K. F. Bohringer , Adv. Mater. 2012 , 24 , 1545 .

[6] Moyuan Cao , Kan Li , Zhichao Dong , Cunming Yu , Shuai Yang , Cheng Song ,Kesong Liu ,
and Lei Jiang, Superhydrophobic “Pump”: Continuous and Spontaneous Antigravity Water Delivery, DOI: 10.1002/adfm.201501320.

[7] Siyuan Xing, Jia Jiang and Tingrui Pan, Interfacial microfluidic transport on micropatterned
superhydrophobic textile, Lab Chip, 2013, 13, 1937.

[8] Ethan Leea, Hongbin Zhang, John K. Jacksonb, Chinten James Limc and Mu Chiao, Janus films with stretchable and waterproof properties for wound care and drug delivery applications, DOI: 10.1039/C6RA16232K

[9] J. S. Boateng, K. H. Matthews, H. N. E. Stevens and G. M. Eccleston, J. Pharm. Sci., 2008, 97, 2892

[10] https://en.wikipedia.org/wiki/Capillary_action

[11] M. Madou, Fundamentals of Microfabrication, CRC Press, 1995.

[12] López-Huerta, Blanca Cervantes, Octavio González, Julián Hernández-Torres, Leandro García- gonzález, Rosario Vega, Agustín L. Herrera-May, Enrique Soto Biocompatibility and Surface Properties of TiO_2 Thin Films Deposited by DC Magnetron Sputtering .1996-1944

[13] Wenzel R N (1936) Resistance of solid surfaces to wetting by water. *Industrial and Engineering Chemistry* 28:988.

[14] Cassie A B D and Baxter S (1944) Wettability of porous surfaces. *Transactions of the Faraday Society* 40:546.

[15] Neinhuis C and Barthlott W (1997) Characterization and distribution of water-repellent, self-cleaning plant surfaces. *Annals of Botany* 79:667.

[16] Ou J, Perot B, and Rothstein J P (2004) Laminar drag reduction in microchannels using ultrahydrophobic surfaces. *Physics of Fluids* 16:4635.

[17] Lafuma A and Quéré D (2003) Superhydrophobic states. *Nature Materials* 2:457.

[18] Jung Y C and Bhushan B (2008) Wetting behavior during evaporation and condensation of water microdropss on superhydrophobic patterned surfaces. Journal of Microscopy 229:127.

[19] H. Kusumaatmaja, M. L. Blow, A. Dupuis and J. M. Yeomans, The collapse transition on superhydrophobic surfaces, Europhys Lett., 81 (2008) 36003.

[20] Luo, C., Xiang, M., Liu, X., and Wang, H. Transition from Cassie-Baxter to Wenzel States on Microline-formed PDMS Surfaces Induced by Evaporation or Pressing of Water Dropss. *Microfluidics and Nanofluidics* 2011, *10*, 831-842.

[21] He B, Patankar N A, and Lee J. (2003) Multiple Equilibrium Drops Shapes and Design Criterion for Rough Hydrophobic Surfaces. *Langmuir* 19:4999.

[22] Nosonovsky M and Bhushan B (2007) Hierarchical roughness optimization for biomimetic superhydrophobic surfaces. *Ultramicroscopy* 107:969.

[23] Quéré D and Reyssat M (2008) Non-adhesive lotus and other hydrophobic materials. *Philosophical Transactions of the Royal Society A* 366:1539.

[24] Park C I, Jeong H E, Lee S H, Cho H S, and Suh K Y (2009) Wetting transition and optimal design for microstructured surfaces with hydrophobic and hydrophilic materials. *Journal of Colloid and Interface Science* 336:298.

[25] Liu X and Luo C (2010) Fabrication of Super-hydrophobic channels. *Journal of Micromechanics and Microengineering* 20:025029.

[26] Yoshimitsu Z, Nakajima A, T. Watanabe T, and K. Hashimoto K (2002) Effects of surface structure on the hydrophobicity and sliding behavior of water dropss. *Langmuir* 18:5818.

[27] Adamson A V (1990) *Physical Chemistry of Surfaces* (New York: Wiley).

Biographical Information

Manasvikumar Oza has received a Bachelor's of Engineering Degree in Aeronautical Engineering from Sardar Vallabhbhai Patel Institute of Technology, Gujarat Technological University, India in May 2014. During his undergraduate studies, he was involved in various organizations and he was awarded as successful organizer for organizing national level technical events. His project ideas were very intellectual and his project on "CFD analysis for high-lift configuration to capture aerodynamic coefficient" was highly appreciated by professors. His capstone project was "Numerical analysis over variable sweep wing in micro air vehicle" and he published a paper in ITMAE 2014 on this project. He worked as a Mechanical Design Engineer Intern. He has been a Graduate Student in the Mechanical & Aerospace Engineering Department at UT Arlington since January 2015. He joined Dr. Cheng Luo's group in April 2015 and work with his group on self-transport of liquid drops through a functional mesh for removing sweat away from skin. His interests are majorly, CAD design and simulation, medical devices manufacturing and mechanical design.